Analog Integrated Circuits and Signal Processing (2025) 124:54
https://doi.org/10.1007/s10470-025-02429-6

Fuel cell EV for smart charging with stochastic network planning using hybrid EOO-SNN approach

S. Dhas Bensam[1] · K. S. Kavitha Kumari[2] · Amarendra Alluri[3] · P. Rajesh[4]

Received: 17 January 2024 / Revised: 28 April 2025 / Accepted: 12 May 2025 / Published online: 7 July 2025

Abstract
This paper proposes a hybrid method for network expansion planning for electric vehicle charging stations. The hybrid method is the combination of Eurasian Oystercatcher optimizer (EOO) and spiking neural network (SNN) approach and is usually referred as EOO-SNN approach. The major purpose of the work is to extend the optimal charging strategy for EVs, which includes the allocation of charging resources to decrease the charging costs, increase the charging efficiency, and decrease the impact on the power grid. The EOO is used to optimize various aspects, such as charging time, charging station placement, and network expansion planning. The ideal solution is predicted using the SNN. The approach also combined with smart grid technologies, such as demand response mechanisms and fuel cell integration with battery energy storage system, to optimize the energy system and ensure efficient and sustainable EV charging. The proposed method supports scalability/adaptability in EV charging systems, effective charging strategy formulation, and worldwide optimisation of charging infrastructure growth. The proposed method's effectiveness is then evaluated on the MATLAB platform and compared to other existing approaches. The efficacy of the proposed system is high as 45%.

Keywords Smart charging · Fuel cell · Electric vehicle · Stochastic planning · Distributed network · Battery storage · Smart grid

1 Introduction

Recent advancements in electric mobility, distributed energy technologies, and smart grid infrastructures have significantly transformed the landscape of urban energy systems [1]. Electric Vehicles (EVs), supported by intelligent charging infrastructure and vehicle-to-grid (V2G) capabilities, have evolved from simple transportation tools into dynamic components of modern power systems [2]. Simultaneously, the development of microgrids (MGs) equipped with renewable energy sources like wind turbines, solar panels, microturbines, and battery energy storage systems (BESS) has enabled localized, resilient, and flexible power management [3, 4]. These innovations not only enhance energy efficiency but also support decarbonization goals in line with global climate policies [5, 6].

Despite these technological strides, the large-scale integration of electric vechicles and their charging stations (EVCS) into power distribution networks poses new challenges [7]. The transportation sector remains a major contributor to carbon emissions and urban air pollution, urging a shift toward sustainable mobility solutions [8]. As EV adoption rises, so does the demand for accessible, high-capacity charging infrastructure. Planning the optimal location, sizing, and scheduling of EVCS requires a holistic approach that considers grid capacity constraints, stochastic EV user behavior, traffic flow dynamics, and energy availability from local DERs [9]. Moreover, uncoordinated charging

✉ S. Dhas Bensam
dhasbensam0629@gmail.com

K. S. Kavitha Kumari
kavithakseee@gmail.com

[1] Electrical and Electronics Engineering, V S B College of Engineering, Technical Campus, Coimbatore, Tamil Nadu, India

[2] Assistant Professor Grade-II, Department of Electrical and Electronics Engineering, Aarupadai Veedu Institute of Technology, Vinayaka Mission's Research Foundation, Paiyanoor, Tamil Nadu, India

[3] Electrical and Electronics Engineering, S R Gudlavalleru Engineering College, Krishna, Andhra pradesh, India

[4] Research and Development, Xpertmindz Innovative Solutions Private Limited, Kuzhithurai, Tamil Nadu, India

can lead to grid congestion, reliability issues, and increased operational costs [10, 11]. Therefore, a coordinated and forward-looking planning framework is essential to balance energy supply and demand while ensuring system reliability and economic feasibility [12, 13].

Many research works have earlier presented in the literatures which are depends on the applying numerous technqiues and features. Few of them are reviewed here.

Jian et al. [14] suggested a stochastic p-robust optimisation approach (SPROT) for designing off-grid charging stations for electric and hydrogen cars powered by solar and hydrogen storage systems. The suggested approach optimized the system's performance under uncertainty. Nonetheless, the impact of local environmental factors on the PV system was not considered.

Jouda et al. [15] suggested a deep stochastic reinforcement learning technique for energy management strategies in fuel cell hybrid electric vehicles (FCHEVs) facing epistemic uncertainty. The authors showed that their approach outperformed existing methods, achieving notable advancements in fuel economy and reducing training time compared to traditional strategies.

Sivaram Krishnan et al. [16] developed a hybrid SHO-CSGNN method for fuel cell electric vehicle power management that combines the Contrastive Self-Supervised Graph Neural Network (CSGNN) with the Sea-Horse Optimisation Algorithm (SHO). The suggested method demonstrated reduced computation time and improved energy efficiency, outperforming conventional algorithms such as SSA, FFA, and GA in terms of time efficiency and performance.

Balakumar et al. [17] suggested a Bidirectional Long Short-Term Memory (B-LSTM) model for dynamic pricing and scheduling EV charging in distribution networks. By integrating this model with demand response programs, they achieved optimal peak demand management, reducing grid congestion and optimizing EV charging efficiency based on feeder-wise electric consumption forecasts.

Aljafari et al. [18] presented a Multi-Agent Deep Neural Network (MADNN) approach to optimize the charging and discharging of EV, minimizing operational costs while improving electricity pricing. Their study demonstrated significant savings and reduced network convergence time, making the approach suitable for large-scale implementation.

Yao et al. [19] introduced a multi-objective robust optimization framework for smart discharging and charging of electric vehicles in smart cities. By incorporating demand response strategies, their model improved clean energy utilization and optimized charging costs, providing a robust solution for urban environments with uncertain energy loads.

Chatterjee et al. [20] developed a Bi-LSTM predictive control-based energy management system for fuel cell hybrid electric vehicles. The system outperformed traditional methods in terms of energy utilization and environmental impact, offering a significant reduction in emissions while enhancing fuel economy.

Aljohani et al. [21] suggested a tri-level hierarchical optimization framework for the coordinated control of large-scale EV charging. Utilizing a Stackelberg leader–follower model, the approach effectively optimized energy consumption and operational costs across multiple levels, offering a robust solution for managing the widespread integration of EVs.

Lan et al. [22] employed machine learning techniques to optimize energy management in renewable microgrids, particularly focusing on the charging demands of HEVs. Their implementation of the Dragonfly Optimization Algorithm resulted in a 2.5% reduction in operational costs, highlighting its potential to enhance energy efficiency in microgrid systems with HEV integration. Table 1 shows the table of literature comparisons.

Several studies have focused on optimizing the operation and planning of Electric Vehicle Charging Stations (EVCS) and their integration with power grids. One method plan off-grid charging stations for electric and hydrogen cars fed by solar and hydrogen storage systems using a stochastic p-robust optimisation strategy. While it optimized system performance under uncertainty, it did not consider the environmental impacts on photovoltaic system efficiency. Another study employed a deep stochastic reinforcement learning approach for energy management in fuel cell hybrid electric vehicles (FCHEVs), showing significant improvements in fuel economy and reduced training time, but it did not explore integration with the grid or EVCS. A hybrid Sea-Horse Optimization and Contrastive Self-Supervised Graph Neural Network (SHO-CSGNN) method for power management in fuel cell electric vehicles (FCEVs) reduced computation time and improved energy efficiency, yet it did not address the broader integration of EVs with charging stations or grids. Bidirectional Long Short-Term Memory (B-LSTM) models for dynamic pricing and scheduling in EV charging reduced grid congestion and optimized peak demand management but focused solely on distribution networks without incorporating renewable energy sources or microgrid integration. The Multi-Agent Deep Neural Network (MADNN) strategy for optimizing the discharging and charging of EVs minimized operational costs and improved electricity pricing, but it did not consider renewable energy integration or microgrid coordination. A multi-objective robust optimization framework for smart charging and discharging in smart cities improved clean energy utilization and reduced charging costs but lacked flexibility at

Table 1 Table of literature comparisons

Reference	Objective	Methodology	Key outcomes	Limitations
Jian et al. (2020) [14]	To optimize planning of off-grid EV and hydrogen vehicle charging stations	Stochastic p-robust optimization (SPROT)	Enhanced planning under uncertainty for PV and hydrogen storage-based stations	Environmental impacts on PV efficiency not considered
Jouda et al. (2021) [15]	To improve energy management in FCHEVs under uncertainty	Deep stochastic reinforcement learning	Better fuel economy and shorter training times	Limited to vehicle-side EMS; no grid or station integration
SivaramKrishnan et al. (2022) [16]	To enhance energy efficiency in FCEVs through hybrid learning	Hybrid SHO-CSGNN (Sea-horse optimization and contrastive self-supervised graph neural network)	Reduced computation time and improved energy performance	No consideration of EV charging station-level or grid-scale planning
Balakumar et al. (2022) [17]	To manage peak demand and optimize EV charging	Bi-directional LSTM with demand response integrated for pricing and scheduling	Reduced peak load and improved feeder-level efficiency	Focused only on distribution network; lacks renewable energy integration
Aljafari et al. (2022) [18]	To reduce costs in EV charging/discharging using intelligent control	Multi-agent deep neural network (MADNN)	Minimized operational costs and convergence time	No interaction with renewable DERs or microgrid coordination
Yao et al. (2023) [19]	To enable robust EV charging in smart cities	Multi-objective robust optimization with demand response strategies	Better clean energy usage and optimized cost	Lacks flexibility at microgrid scale; uncertainty handling can be more dynamic
Chatterjee et al. (2023) [20]	To design a predictive EMS for FCHEVs	Bi-LSTM-based predictive control	Reduced emissions and enhanced fuel economy	Does not address EV charging stations or grid integration
Aljohani et al. (2023) [21]	To coordinate large-scale EV charging	Tri-level hierarchical optimization (Stackelberg leader–follower model)	Efficient energy and cost management across layers	Not adaptable to real-time renewable generation changes
Lan et al. (2023) [22]	To manage HEV charging in renewable-based microgrids	Machine learning with dragonfly optimization algorithm	2.5% operational cost reduction	Targeted only at HEVs; lacks scalability and integration for broader EVCS systems
Proposed study	To optimize EVCS placement, scheduling, and resource allocation in microgrids with renewables and V2G	Hybrid EOO-SNN approach combining Eurasian oystercatcher optimizer with spiking neural networks	45% improvement in charging efficiency, reduced waiting time, enhanced grid stability	Requires real-time coordination across grid and traffic layers; future work includes real-time validation

the microgrid scale and needed better dynamic uncertainty handling. A Bi-LSTM predictive control system for energy management in FCHEV outperformed traditional methods in terms of energy utilization and emissions reduction but did not address coordination with EVCS or grid integration. A tri-level hierarchical optimization framework for large-scale EV charging coordination, using a Stackelberg leader–follower model, effectively optimized energy consumption and operational costs, though it did not account for real-time changes in renewable energy generation or grid fluctuations. Lastly, a machine learning-based approach optimized hybrid electric vehicle charging in renewable microgrids, reducing operational costs by 2.5%, but was limited by its focus on hybrid vehicles and lacked integration with broader EVCS systems. These above-mentioned research gaps are inspired to do this research work.

The proposed study overcomes existing gaps by integrating a hybrid optimization approach combining the Eurasian Oystercatcher Optimizer (EOO) and Spiking Neural Networks (SNN) to optimize Electric Vehicle Charging Stations (EVCS) within microgrids. Unlike previous methods, this approach effectively integrates renewable energy sources and Vehicle-to-Grid (V2G) technology, ensuring efficient energy management and flexibility. It addresses challenges like EVCS placement, scheduling, and resource allocation by enabling real-time adaptability to dynamic grid conditions, improving resource utilization, and minimizing energy loss. Additionally, the model's scalability allows for application across various urban settings with diverse energy demands, while enhancing grid stability by leveraging bidirectional energy flow through V2G. The study's key advantages include better resource allocation, increased system flexibility, and improved grid reliability, offering a robust and scalable solution for future EVCS development that is more efficient, sustainable, and adaptable than existing methods.

The following are the contributions of the proposed study:

- The study introduces a novel hybrid optimization method combining the EOO and SNN for optimal planning and operation of EVCS within microgrids, addressing the complexities of energy management and EV integration.
- By incorporating V2G technology, the study enhances the flexibility of the grid, enabling bidirectional energy flow and helping stabilize the grid during peak demand periods, a feature not fully explored in existing studies.
- The proposed methodology optimizes the allocation of renewable energy resources, like wind, solar, and battery storage, along with EV charging, thereby reducing energy loss and improving overall efficiency in microgrid systems.
- The study offers a scalable and adaptive solution that can be applied to diverse urban environments with varying energy demands, making it a versatile solution for future EVCS development and smart grid integration.
- The proposed system not only minimizes operational costs but also focuses on environmental sustainability by optimizing clean energy usage, reducing emissions, and improving overall energy efficiency in urban transportation systems.

The remainder of this manuscript is structured as follows: Part 2 shows the configuration of EVCS for planning network, Part 3 shows the reduced the cost using EOO-SNN approach, Part 5 shows the result and discussion, and Part 4 shows the concludes the paper.

2 Configuration of smart charging using fuel cell with battery

The configuration of smart charging using fuel cell with battery is shown in Fig. 1. Battery SOC zone selection in different EMSs is determined empirically; battery efficiency is unaffected in this process. Furthermore, real-time condition and driving cycle comparison have been used to identify driving conditions, and this has allowed for a more effective reduction of FC power fluctuations. An innovative online energy management system (EMS) based on OMC, ECMS, and SMC is offered to regulate energy in fuel cell electric cars. A novel formula for the combined efficiency of batteries, standard deviation, and its expectation is used to determine the Battery SOC categorization. A novel function that is based on demand power, acceleration, and speed separates the vehicle's dynamic behaviour into five stages [23]. In the framework of ECMS software, the values of the hydrogen fuel per energy joule are calculated and formulated while taking into consideration the battery's charging and discharging efficiency. Power requirement and value of hydrogen fuel are used to classify various demand power sectors. Lastly, the dynamic power coefficient technique is used to ensure EMS function and prevent the battery from being overcharged. The proposed technique is used to enhance the charging interval, charging station placement, and network expansion planning and predicts the optimal solution.

The proposed smart charging system integrates fuel cells with batteries to optimize both the discharging and charging cycles of EVs. V2G technology is used, allowing EVs to charge from the grid and discharge surplus energy back into the grid as needed. This bidirectional flow of energy reduces

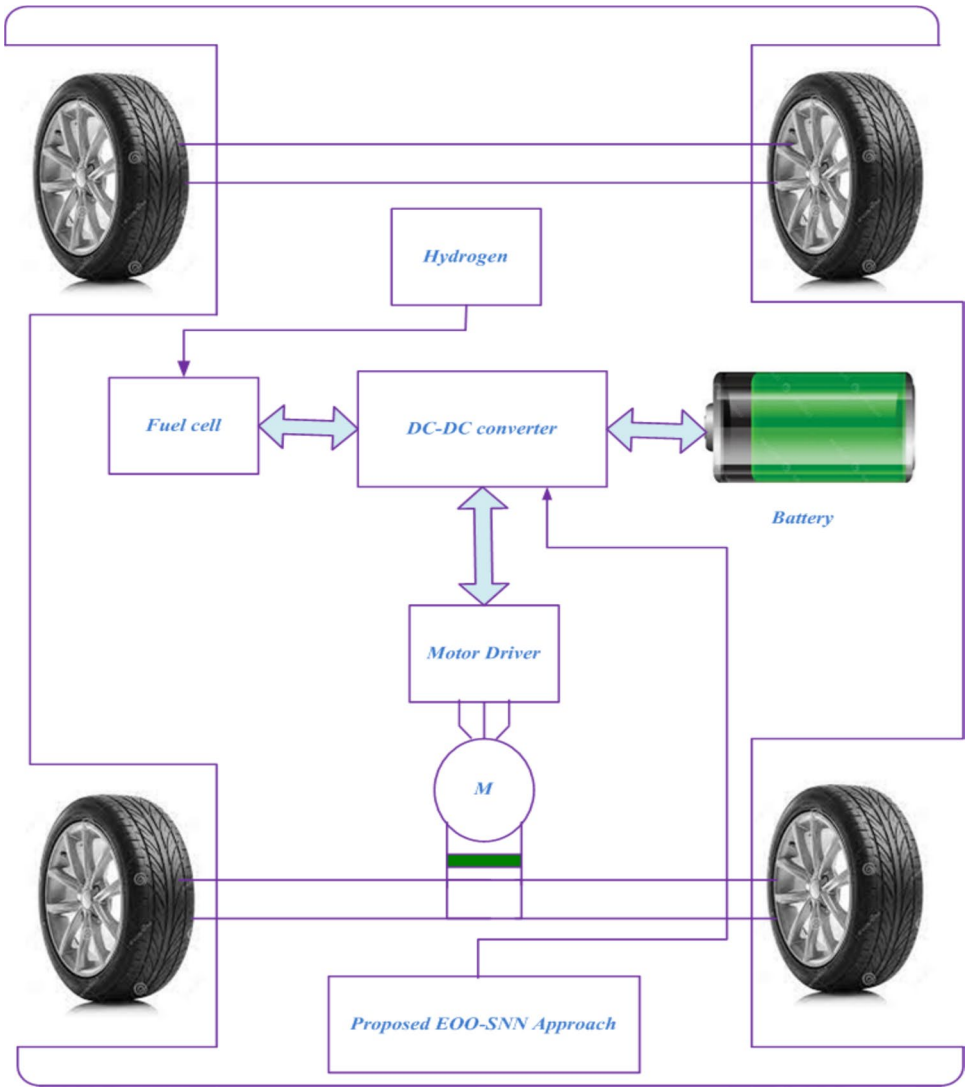

Fig. 1 Configuration of EV smart charging using fuel cell

electricity prices and promotes grid stability by providing a consistent source of stored energy during peak demand periods. The EMS considers the V2G functionality when deciding when to charge and discharge EV batteries, ensuring efficient grid utilization and renewable resource usage while minimizing battery wear.

2.1 Modeling of fuel cell

The fuel cells are electrochemical devices that transform energy from chemicals into electrical energy. The fuel cell model has a variety of components, resulting in an internal voltage drop [24]. A fuel cell's output voltage is depicted in Eq. 1.

$$V_{Fc} = E - (V_{Ohm} + V_{Act} + V_C) \tag{1}$$

here, E indicates the nernst instantaneous voltage, V_{Act} is denoted as the reduced fuel cell activation voltage, V_{Fc} is denoted as the Output voltage of fuel cells, V_{Ohm} is denoted as the ohmic voltage drop, and V_C is denoted as the voltage drop caused by the capacitance created by the two electrodes with opposing polarities within the fuel cell. Equation (2) is used to calculate the fuel-cell M_{H2} power; which link the power P_{Fc} to the mass usage of hydrogen.

$$m_{H2} = \int_0^t \frac{P_{Fc}(t)}{\eta_{Fc} \times \rho_{H2}} dt \tag{2}$$

$$\eta_{Fc} = \frac{P_{Fc}}{P_{H_2}} \tag{3}$$

2.2 Modeling of FCEV

It is crucial to calculate the necessary power in the FC electric car for various driving conditions [25]. Equation (4)

demonstrates that the required performance is dependent on vehicle parameters, acceleration, aerodynamic factors, pitching, and gravity forces.

$$P_{DEMAND} = \frac{V(MA + 0.5\rho C_D A_J V^2 + C_{RR} M\, GCOS\alpha + M\, GSIN\alpha}{\eta_{DRIVERTRAIN}} + P_{AUXILIARY} \tag{4}$$

where, V is the velocity, ρ specifies the air density, C_D denotes the drag coefficienct, A_J specifies the frontal area, C_{RR} represents the rolling resistance coefficient, α specifies the slope, $\eta_{DRIVERTRAIN}$ denotes the drivetrain efficiency, $P_{AUXILIARY}$ is the auxillary power and P_{DEMAND} is the power demand.

2.3 Modeling of battery

Due to its long lifespan and high energy density, the lithium-ion battery is regarded as the optimal solution to other battery types [26]. For the greatest performance, an accurate dynamic battery model that takes internal factors and the amount of charge is necessary. Regenerative braking causes reduction and oxidation reactions that transfer charge to the battery, making it unable to respond to a strong dynamic power profiles. Exposing the battery to such high dynamic profiles might result in cell breakdown and a shorter lifetime. According to the regenerative braking resistance, the regenerative braking system is specifically made to withstand extreme braking situations, which leads to the loss of the largest amount of regenerative braking energy. Equations (5–10)

$$\begin{cases} V_{BAT} = U_{OC} - R_O, \;\; I_{BAT} - V_P \\ V_P \quad\quad = -(1/R_P C_P)\, V_P + (1/C_P)\, I_{BAT} \end{cases} \tag{5}$$

$$SOC = SOC_O - \frac{\int_0^1 I_{BAT}\, DT}{E_{BATT}} \tag{6}$$

where, U_{OC} specifies the battery open circuit voltage, V_{BAT} specifies the Battery cell voltage, R_O specifies the ohmic internal resistance, V_P denotes the polarization voltage, I_{BAT} denotes Battery cell current, R_P is the Polarization resistance and C_P is the polarization capacitance.

The factors that impact how quickly batteries charge and discharge include battery capacity, open circuit voltage, internal battery resistance and state of charge. Battery efficiency and level of charge have a nonlinear relationship as a result of the link between open-circuit voltage and internal resistance.

2.4 Boost converter modeling

The FC system generates variable voltage, with a substantial difference between conditions of full load and empty load. For illustration, a PEMFC has a single-cell voltage of 0.6 V at maximum load and 1.23 V at no load. As a result, the FC requires a DC-DC converter to adjust the output voltage to suit varied operating conditions. It is crucial to keep the current ripple below 5% of the FC's rated current, as FCs are sensitive to current fluctuations [26]. Classical boost converters continue to be used often despite advancements in power electronics technology because of its inexpensive cost, simplicity of design, steady conduction mode input current without pulses, and low component count. However, the voltage gain of these converters is constrained. Figure 2 depicts the circuit of boost converter.

$$N_B = \frac{(1-D)^2 DR}{2F_S} N > N_B \tag{7}$$

here, D specifies the duty cycle, N_B specifies the number of Boost stages, R specifies the converter's output resistance, F_S is the switching frequency and N denotes turns ratio.

$$M_{MIN} = \frac{D\, V_O}{\Delta V\, RF_S} M > M_{\min} \tag{8}$$

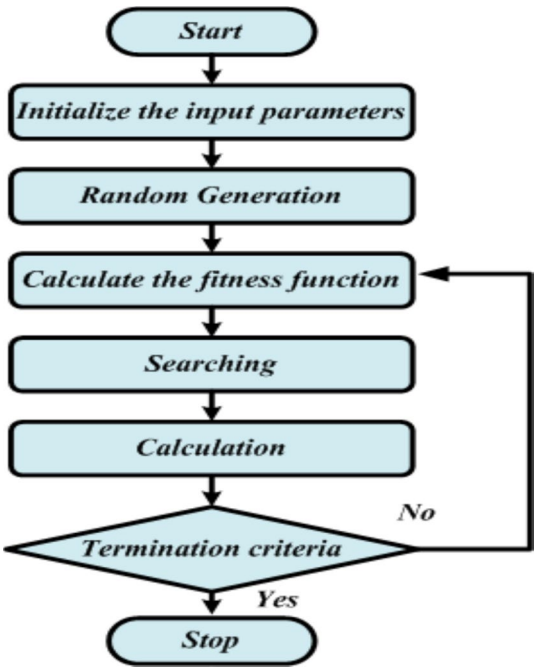

Fig. 2 Flowchart of EOO

where, M_{MIN} is the minimum required voltage gain for proper converter operation, V_O specifies the output voltage, M specifies the Voltage gain of the boost converter.

Where Eqs. (9) and (10) are utilized to calculate the ripple in the output voltage and input current of the converter.

$$\Delta_{IL} = \frac{V_S}{2L}\, DT_S \tag{9}$$

$$\Delta V = \frac{V_S}{2RC} DT_S \tag{10}$$

here, Δ_{IL} specifes the Input current ripple, ΔV denotes the Voltage ripple, C is the Converter capacitor, V_S is the voltage drop and L is the converter inductor.

2.5 Modeling of EV

The EV model replicates the battery's precise behaviour during charging and discharging activities. With V2G (Vehicle-to-Grid) technology, the model allows the vehicle to return energy to the grid when grid demand is high, while also charging during off-peak periods [27]. This bi-directional energy flow impacts the SOC of the battery and contributes to overall battery degradation. The frequency and magnitude of energy cycles discharging and charging affect the battery's performance and longevity. The V2G model optimizes these cycles to strike a balance between providing grid support and minimizing the impact on battery health. The total load, which results from various forces acting on the vehicle, is represented by the following Eqs. (11–15):

$$F_L = F_A + F_R + F_G + F_{ACC} \tag{11}$$

$$\begin{cases} F_A = 0.5\,.\,\phi\,.\,S.C_D.V_{VE}^2 \\ F_R = (M_{EV} + M_{ESS}) \cdot \left(C_0 + C_1 + V_{VE}^2\right) \cdot G \\ F_G = (M_{EV} + M_{ESS}) \sin(\beta)\,.G \\ F_{ACC} = (M_{EV} + M_{ESS})\,.\,(dV_{VD}/dt) \end{cases} \tag{12}$$

here, F_L indicates the load force; F_R indicates the rolling force; F_G denotes the force of gravity; F_{ACC} indicates the force of acceleration; ϕ specifies the electrical density; S specifies the area; C indicates the drag constant; V_{VE} is denoted as the vehicle speed; M_{EV} , M_{ESS} is denoted as the mass of the ESS and EV; G specifies the constant of gravitation. The desired power of an electric vehicle is stated as:

$$\begin{aligned} &P_{EV} \\ &= ((M_{EV} + M_{ACC})\,(dV_{VE}/dt) + F_A + F_R + F_G) \\ &\times V_{VE} \end{aligned} \tag{13}$$

Driving resistances include factors such as Gravitational forces, aerodynamic drag, and rolling resistance. The maximum energy of a battery is established by

$$E_{MAX} = \int_0^T P_{EV}\,(T)\,dt \tag{14}$$

2.6 Problem formulation

The optimal energy management for smart microgrids using EVCS is a multi-objective optimisation issue. The major aim is to reduce overall operational costs while ensuring system dependability and battery health. The proposed system includes Distributed Energy Resources (DERs) like Battery Energy Storage Systems (BESS), Fuel Cells (FC), and renewable sources, with smart coordination of EVs acting as both loads and sources (via V2G).

For example, imagine a small smart microgrid with a fuel cell, a grid connection, and three EVs connected to a charging station. Electricity from the grid is cheaper at night and more expensive during the day. Each EV has a battery that must stay between 30 and 80% charge. In the morning, the EVs arrive with a low battery (around 35%). The EMS charges the EVs during the night when electricity is cheap and allows them to send power back to the grid (using Vehicle-to-Grid or V2G) during the day when prices are high. This way, the system saves money, supports the grid, and keeps the EV batteries healthy by following the SoC and charging limits. This example shows how the model works to manage energy smartly and efficiently.

2.6.1 Objective function

The total cost to be minimized consists of three primary components: the cost of electricity purchased from the utility grid, the generation cost from local DERs, and the battery degradation cost associated with V2G operation:

$$T_C = \min \sum_{t=1}^{T} \left(A_t.P_{grid,t} + \sum_{i=1}^{N} C_i\,(P_{DG,t}) + C_{\deg}\,(E_{V2G,t}) \right) \tag{15}$$

where, A_t specifies the grid electricity price at time t [$/kWh], $P_{grid,t}$ specifies the power purchased from the grid [kW],$C_i\,(P_{DG,t})$ denotes the generation cost of the ith distributed generator and $C_{\deg}\,(E_{V2G,t})$ represents the battery degradation cost based on V2G usage.

The inclusion of V2G technology enables electric cars to discharge energy back into the grid during peak demand and charge during off-peak hours. This bi-directional flow of energy not only optimizes grid usage but also contributes to

minimizing electricity costs and grid dependency [28]. V2G is modeled in the objective function as an additional cost associated with battery degradation due to frequent cycling, as this impacts the long-term performance of EV batteries. Battery degradation is modeled as a linear function of energy discharged back to the grid, with an assumed end-of-life cycle after 5000 charge–discharge cycles. The degradation cost reflects the balance between economic benefit and the potential degradation of EV batteries, ensuring a fair and sustainable participation in V2G schemes.

2.6.2 Constraints

The proposed optimization model includes several operational and technical constraints, which are described below:

- The technical constraints of the DG units

$$A_{\min,\,n} \le A_n \le A_{\max,n}\ i = 1.....N_{DG} \tag{16}$$

where, $A_{\min}$ and $A_{\max}$ specifies the maximum and minimum of the electrical technical process, in that order. These constraints ensure that each DG unit operates within its technical capability.

- The SoC constraint:

$$for\ i = 1.....N\ \ SoC_{\min} \le SOC_N \le SOC_{\max} \tag{17}$$

This constraint maintains the battery health of the EVs by limiting the state of charge. In this work, the smallest and highest SoC are set to 30% and 80% of the battery's capacity, in that order, to prevent premature aging and extend battery life.

- The average discharge and charge of batteries is reserved as follows:

$$for\ h \in C\ 0 \le P\,(h) \le F_{\max} \tag{18}$$

here, h indicates the duration of a day, $P\,(h)$ represents the rate of charging and discharging for hour, C denotes the duration of the window for charging, and $F_{\max}$ indicates denotes the highest charging rate that the EV charger can provide.

- Velocity constraint:

$$V_{\min} \le v\,(t) \le V_{\max},\ \forall t \tag{19}$$

The velocity of the vehicle is constrained between $V_{\max}$ and $V_{\min}$ specifies the maximum and minimum allowable velocities (based on road and safety conditions), $v\,(t)$ is the velocity at time t. This constraint ensures safe and realistic vehicle operation aligned with traffic and driving behavior.

3 Reduced the cost using EOO-SNN algorithm

The optimal charging strategy is an important factor for the EV charging. The EOO is used to find the optimal solution which is optimally predicted by the SNN method. The complete clarification of the EOO-SNN approach is designated in the below sections.

3.1 Eurasian oystercatcher optimizer (EOO) algorithm

The Eurasian oystercatcher optimizer algorithm simulates the eating habits of Eurasian oystercatchers to find mussels [29]. The fundamental purpose of EO is to maintain a balance between their calories and the energy derived from mussel.

Step 1. Initialization.

Initialise the oystercatcher's input variables using the goal function's factors.

$$X_1\,(i\ =\ 1,\,2,\,.....,\,n) \tag{20}$$

where, X_1 specifies the position vector of the i^{th} search agent.

Step 2. Random generation.

Following initialisation, random vectors produce the input variables at random.

$$e\ =\ \begin{bmatrix} Y_{11} & Y_{12} & Y_{13} \\ Y_{21} & Y_{22} & Y_{23} \\ Y_{31} & Y_{32} & Y_{33} \end{bmatrix} \tag{21}$$

here, e is the random generation and Y specifies the set of objective function.

Step 3. Fitness calculation.

The objective function determines fitness. The fitness calculation is done by each search agent of the EO.

$$F(t) = Min\ (T_C) \tag{22}$$

where, $F(t)$ is the fitness value at iteration t.

Step 4. Searching the mussels.

The objective of the EO is to maintain equilibrium between the energy and calories derived from the mussels. The height of the mussels is directly correlated with energy and calories. Both the number of calories and the required opening time grow with the height of the spherical tank. Therefore, excessive energy is required for EO waste. The EO's actions during the search process are depicted as follows:

$$Z = T + F + H * e * (Y_{best} - Y_{t-1}) \tag{23}$$

$$Y_t = Y_{t-1} * C \tag{24}$$

here, Z is specified as the EO's final energy in every repetition, Y_t is denoted as the location of the mussels, H is specified as the height of the mussels, T is specified as the duration needed to access the existing solution, e specifies the arbitrary value, C specifies the caloric value, F is denoted as the energy.

Step 5. Calculation based on search agent.

To compute the time, energy, and height, use the previous step's search agent. Equations (25–27)

$$T = \left(\left(\frac{H-3}{5-3}\right) * 10\right) - 5 \tag{25}$$

$$F = \left(\frac{t-1}{n-1}\right) - 0.5, \text{where } t > 1 \tag{26}$$

$$C = \left(\left(\frac{H-3}{5-3}\right) * 2\right) + 0.6 \tag{27}$$

Based on the calculations shown above, update the best solution.

Step 6. Termination.

In the termination criteria, check the end criteria, and if the best answer is found, the method stops; otherwise, proceed to step 3. Figure 2 shows Flowchart of EOO.

3.2 Prediction based spiking neural network (SNN)

All neural networks that coordinate the beginning of time regardless of the neuronal and synaptic states are included in the phrase"spiking neural network,"which is used in the context of labor. Specifically, during the learning stage of the SNN approach, the synaptic weight can be spontaneously altered by the SNN computation. Based on a large amount of application data, SNN is a superior solution model for balancing exploration and exploitation [30]. The neural code refers to the scheme that spike trains use to display information. The techniques for encoding genuine qualities contain rate encoding, populace encoding, and transient encoding. In a fleeting neural code plan pertinent to classify modeling and predicting activities is assessed to exploit the connected transient occasions concealed inside the succession. It incorporates time to next spike and probabilistic encoding. It keeps adding data to the network by utilizing the exact timing of the spikes. Terminating time series are used to handle spiking neuron input and output, which is referred to as a spike train. The dynamic variable incorporates the upcoming spikes and represents the potential of a spiking neuron. Fresher spikes have a larger effect on net activity potential than do more experienced spikes. If the total sum of the incoming spikes exceeds a predefined value, the neurone fires the spike. Being a dynamic system, SNN's adaptability is a key characteristic for online load forecasting.

In the proposed EOO-SNN-based optimization model, the key parameters are bounded to ensure efficient and effective optimization. For the EOO, the population size (N) ranges from 30 to 100, with a fixed value of 50, and the maximum iterations (MaxIter) are between 50 and 200, set to 100. The mussel length (L) varies from 2 to 10, with a range of [3, 7], while energy values (E) range from 0.2 to 1.0 and −1.0 to 0.0. The time to open mussel (T) is dynamically adjusted based on length, and caloric value (C) is constrained between 0.5 and 3.0. For the SNN, the leak factor (λ) ranges from 0.5 to 1.0, with a set value of 0.9, while the threshold (v) is between 0.5 and 1.5. The time constant (τ) is between 10 and 50 ms, with a fixed value of 20 ms. The time step (Δt) ranges from 0.5 ms to 5 ms, and the learning rate (η) spans from 0.001 to 0.1, set at 0.01. Batch size ranges from 16 to 128, and the number of timesteps varies from 5 to 200, depending on the task. These parameter boundaries ensure an optimal and practical search space for EV charging station network expansion.

4 Results with discussion

This section demonstrated the efficiency of the proposed technique according to the simulation outcome [31]. This work's recommended technique aims to maximise the efficiency of charging resources. The proposed approach is implemented on the MATLAB platform and compared to other current techniques.

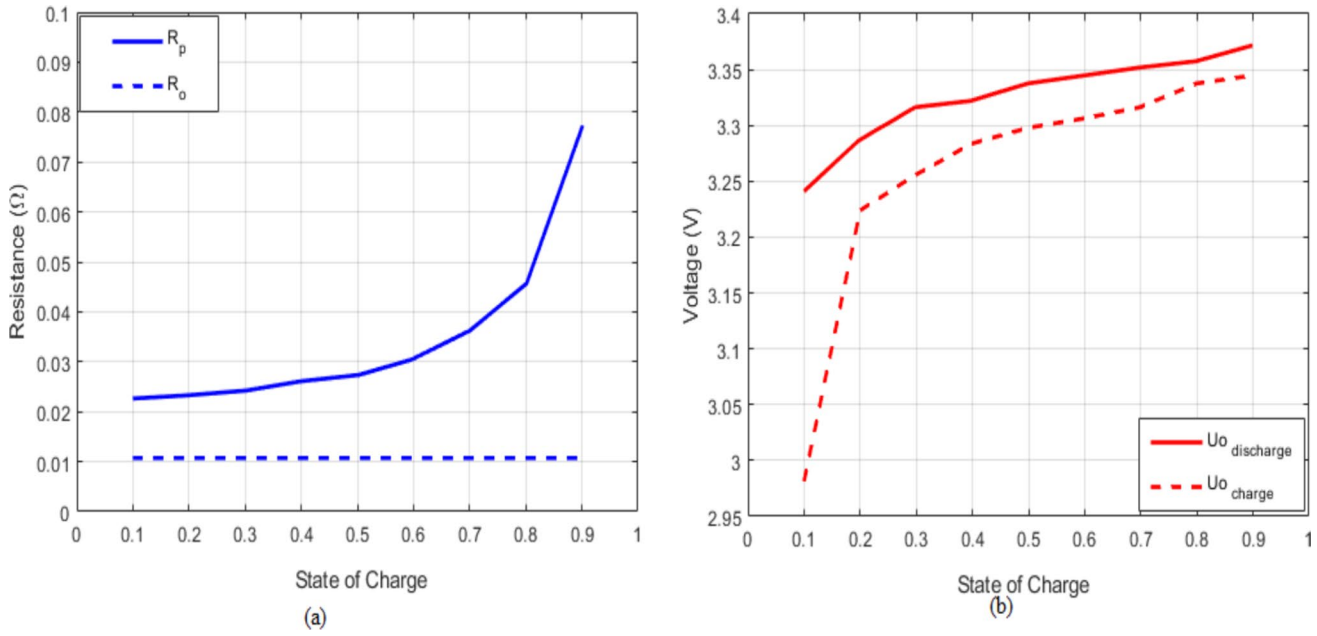

Fig. 3 Analyses of battery parameters **a** resistance **b** voltage

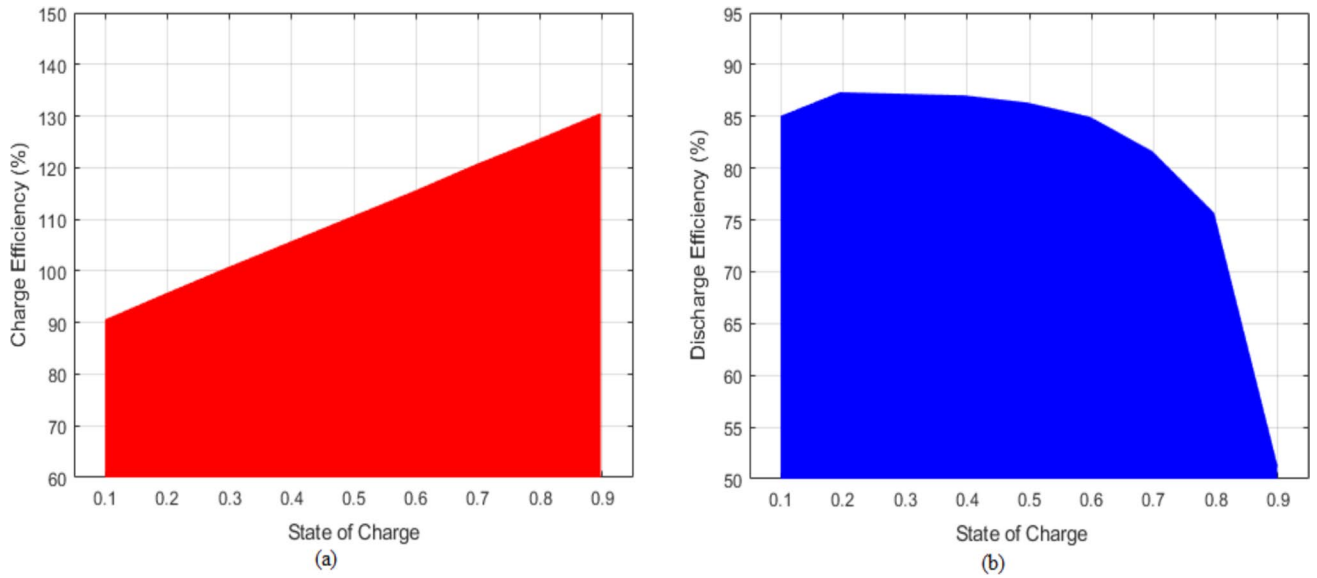

Fig. 4 Analyses of efficiency for battery power **a** charge efficiency **b** discharge efficiency

This section is based on the efficacy of the proposed system based on the EV charging system with fuel cell and battery. Figure 3 shows the battery parameters. Subplot 3(a) shows the battery resistance. The constant pulse test shows the resistance value, that starts at 0.021 Ω at 0.1 SoC and increases to 0.078 Ω at 0.9SoC. Then the constant pulse rate is occurred in the 0.01 Ω at 0.01 to 0.9. Subplot 3(b) shows the voltage for battery. The voltage of battery charge starts in 2.99 V at 0.1 and increases to 3.23 V at 0.2. Again the voltage is raises to 3.345 V at 0.9. The voltage of the battery discharge starts at 3.245 V and ends at 3.375 V. Figure 4 shows the analysis of efficiency for battery power. Subplot 4(a) shows the analysis of charging efficiency for battery power. The charge efficiency is 90% to 130% at 0.1 to 0.9 SOC. Subplot 4(b) shows the discharging efficiency for battery power. The battery power is discharged efficiency from the 85% to 50% at 0.1 to 0.9. The values come from testing the battery's resistance in various scenarios as well as the continuous current pulse test. Figure 5 shows the analysis of battery combined efficiency (BCE) with battery operational regions. The BCE is starts at 88% and decreases to 66% at 0.1 to 0.9. The media of BCE is constant at 87%. The

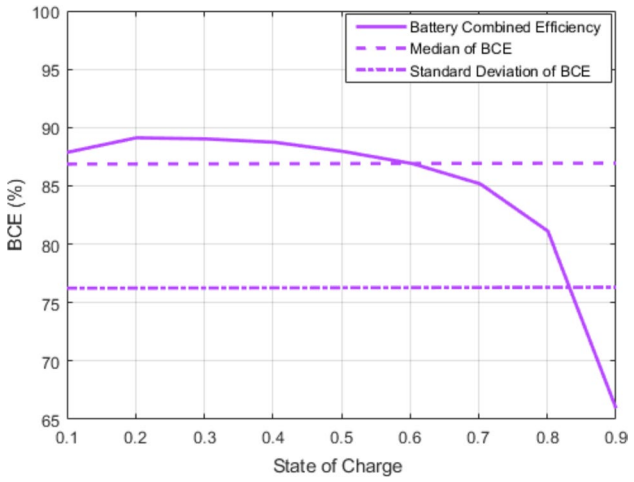

Fig. 5 Analyses of battery combined efficiency with battery operational regions

standard deviation of BCE is constant at 76. BCE reaches its maximum of 88.36% at the 0.2 charge threshold. However, the minimal BCE is attained at the 0.9 charge threshold. BCE has a standard deviation of 7.43% and a median of 87.09%. The SOC regions are distinguished using this data, and the proposed output formats for OMCS are modified taking battery SoC categorization into account. Figure 6 shows the Analyses of PEMFC. Subplot 6(a) portrays the PEMFC voltage. The voltage starts at 1.75 V at zero and decreases to 1.09 V at 1.08 A. Subplot 6(b) portrays the power of PEMFC. The power begins at 0.15 W at zero and raises to 1.1 W at 1.05 A. The utility of hydrogen fuel in the generation of electricity must be ascertained to implement the idea of minimizing fuel usage and make appropriate use of the ECMS concept. Figure 7 shows the Analyses of boost converter. Subplot 7(a) shows the efficacy of the converter. The converter efficacy starts at 97% and decreases to zero at one. Subplot 7(b) shows the gain of the converter. The PEMFC's maximum output power is utilised to determine the effectiveness and dynamic yield of the non-isolated boost converter. Figure 8 portrays the analyses of efficiency. Subplot 8(a) shows the FC stack efficiency. The stack efficiency starts at zero and increases to 60% at 0 to 1 W. Subplot 8(b) portrays the converter efficiency. The converter efficiency starts at 100% and decreases to zero at 0.99 W. The FC system efficiency is shown in subplot 8(c). The efficiency starts at zero and increases to 47% at 1 W. As demonstrated, the efficacy of the non-isolated boost converter decreases as the PEMFC stack's power output increases. The non-isolated boost converter and PEMFC stack have the specified efficiencies. Figure 9 shows the Analyses of hydrogen FC. The hydrogen fuel value (HFV) is calculated as U-shaped curve. The HFV starts in 1.87 at 0.1 W and ends in 1.94 at 1 W, then the lower curves as 1.47 at 0.41 W. The minimum value starts in 1.74 at zero and ends in 1.78 at 1 W. The mean value is in 1.6 to 1.66 at 0 to 1 W. The std. deviation is in 1.48 to 1.52 at 0 to 1 W. A minimum of $1.467 \times 10 - 5$ g/J of hydrogen has been used, with an energy density of 0.4 pu. Operating the fuel cell at 0.8 pu ensures that the hydrogen use per joule equals the mean value of the desired specified region. The HFV standard deviation falls and rises between 0.5 and 0.9 pu. As a result, these are the dispersion, average, and optimal locations that were chosen. In addition, the separation of the eight PEMFC operating modes takes into account the maximum output power, off mode, and a few additional intervals of time. Figure 10 portrays the Analyses of battery equivalence HFV. The equivalent HFV begins at 1.6×10^{-5} at 0.1 and increases to 1.85×10^{-5} at 0.95. The minimal equivalent hydrogen fuel values for FCEVs for each SOC,

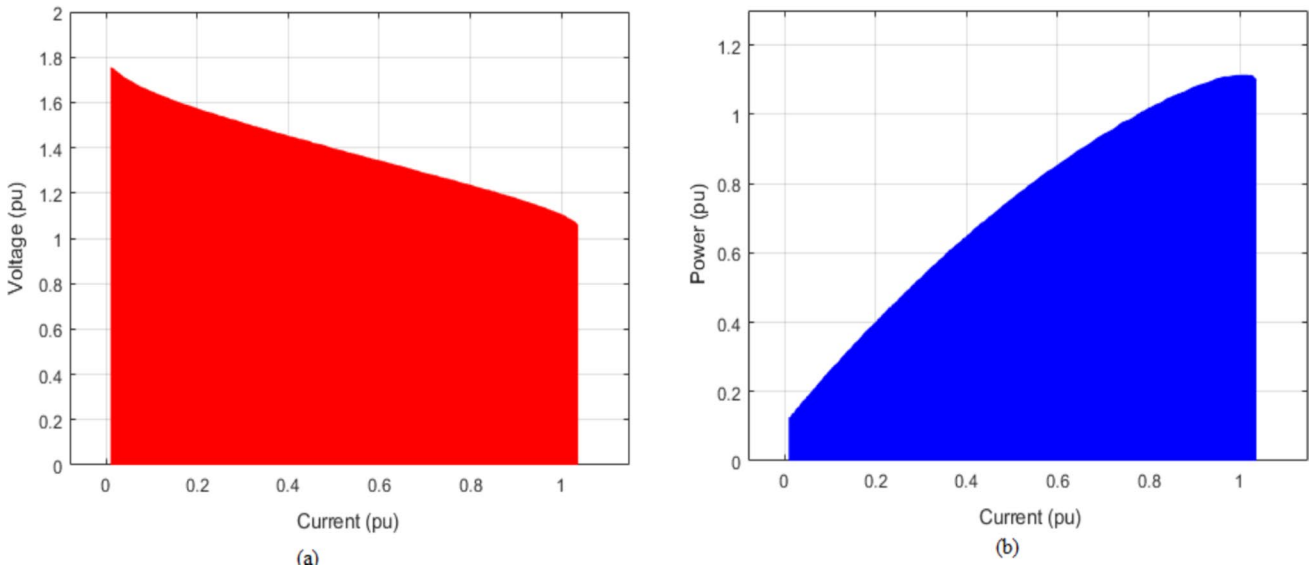

Fig. 6 Analyses of PEMFC **a** voltage **b** power

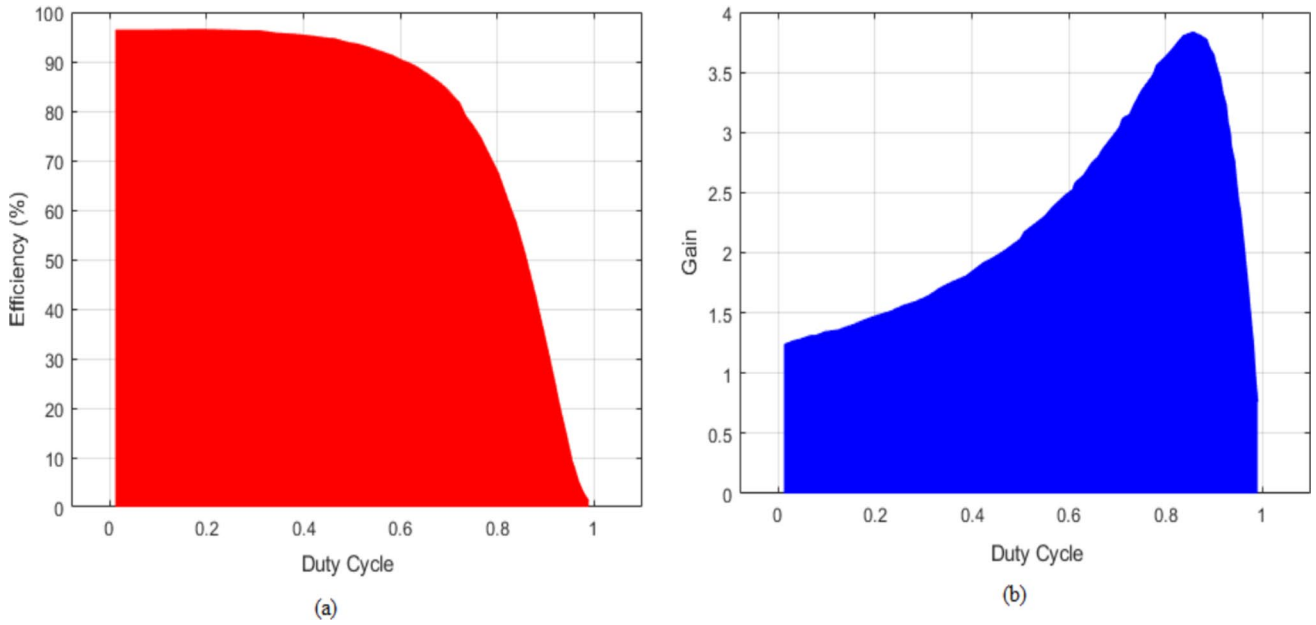

Fig. 7 Analyses of boost converter **a** efficiency **b** gain

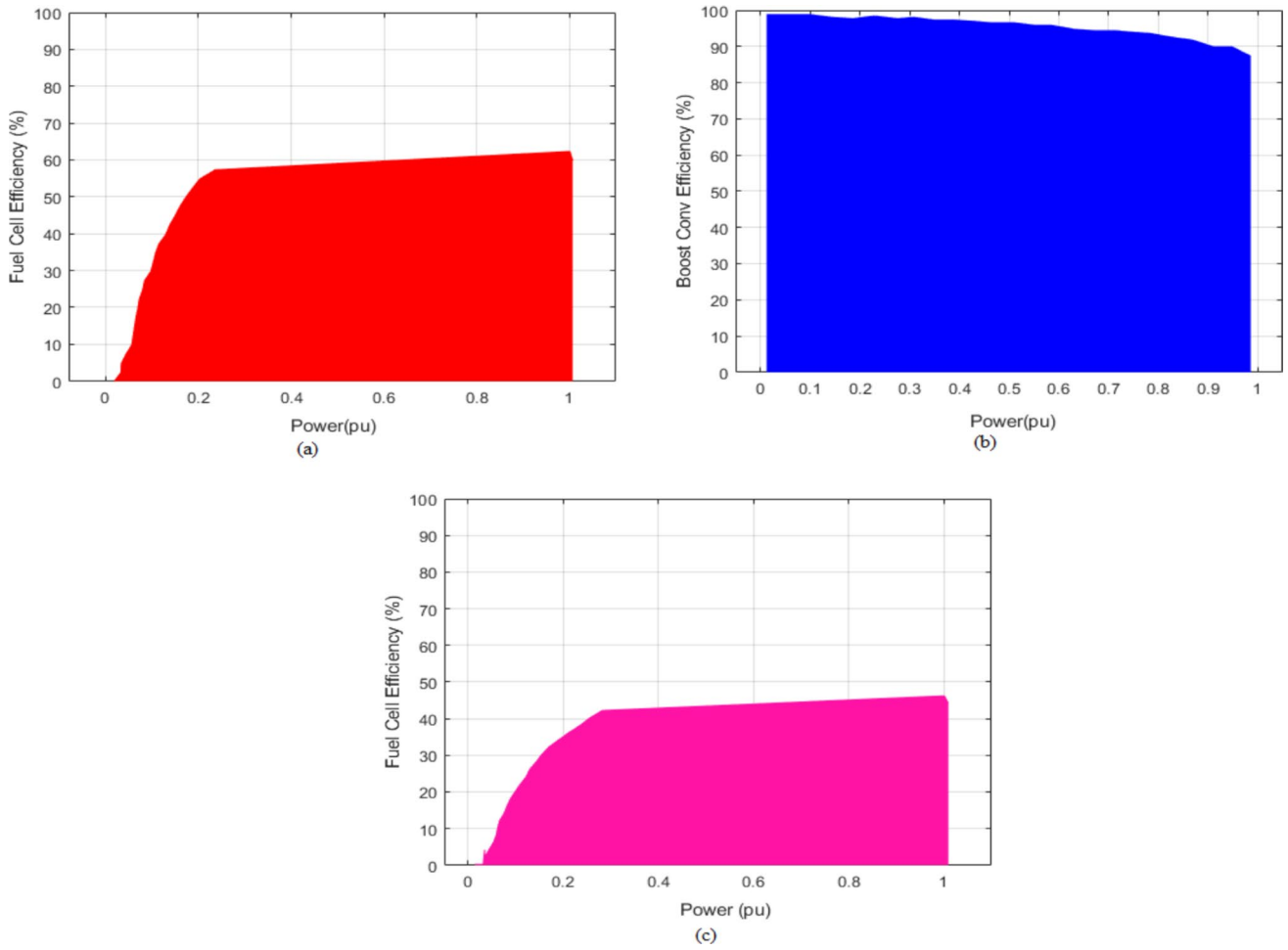

Fig. 8 Analyses of efficiency **a** fuel cell stack efficiency **b** boost converter efficiency **c** fuel cell system efficiency

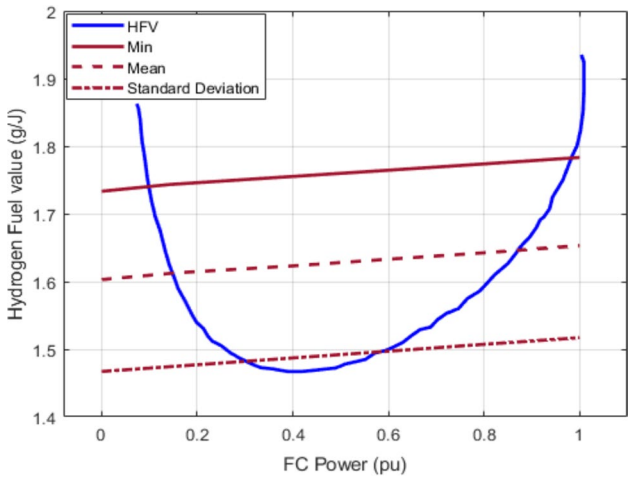

Fig. 9 Analyses of hydrogen fuel cell

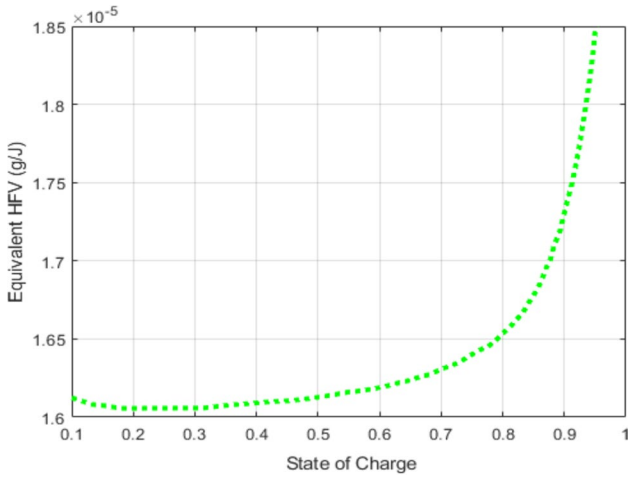

Fig. 10 Analyses of battery equivalent HFV

are expressed in g/J. All SOCs have a decreased equivalent consumption rate at about 0.4 pu for the FC output power, according to the numerical data, when compared to earlier output powers.

Figure 11 shows the Analyses of drive. Subplot 11(a) shows the velocity of the drive. The velocity starts at zero and ends at 1400 s. The velocity is reached 12 V at 200 s, 17 V at 500 s, 11 V at 700 s, 19 V at 900 s, and 14 V at 1100 s. Subplot 11(b) depicts the demand power of drive. The power starts and ends at zero, the power is oscillates among −11 kW to 10 kW. Figure 12 shows the battery SoC. Subplot 12(a) The battery SoC begins at 71.5% and increases to 72.4% at 1400 s, with intermediate values of 73.2% at 350 s and 71.4% at 500 s. Subplot 12(b) The SoC drive begins at 20%, increases to 20.85% at 128 s, and ends at 20.8% at 195 s, with a value of 20.48% at 55 s. Figure 13 portarys the analyses of PEMFC system output power. Subplot 13 (a) The output power of the PEMFC system oscillates between 0.35 kW and 4.8 kW over the time period from 0 to 1400 s. Subplot 13(b) In the PEMFC drive system, the output power remains constant at 2.5 kW from 0 to 199 s. Figure 14 shows the Analyses of FC. Subplot 14(a) portrays the drive velocity of the FC. The velocity begins at zero and ends at zero. The velocity in 5 V at 20 s, in 9.6 V at 50 to 95 s, 14.2 V at 115 s to 170 s. Subplot 14(b) portrays the demand power. The power begins at 0.1 and ends at 0.1 W. The power is oscillated among −2.1 V to 8.1 V at 0 to 195 s. Figure 15 shows a histogram of the monthly operating cost when V2G is used. The x-axis shows the cost values (from about 5670 to 5770), and the y-axis shows how often those costs occur. Most of the cost values are grouped between 5710 and 5720, which means these are the most common and likely costs. Some costs like 5700 and 5730 also appear fairly often, while very low or very high costs are rare. This pattern shows that V2G

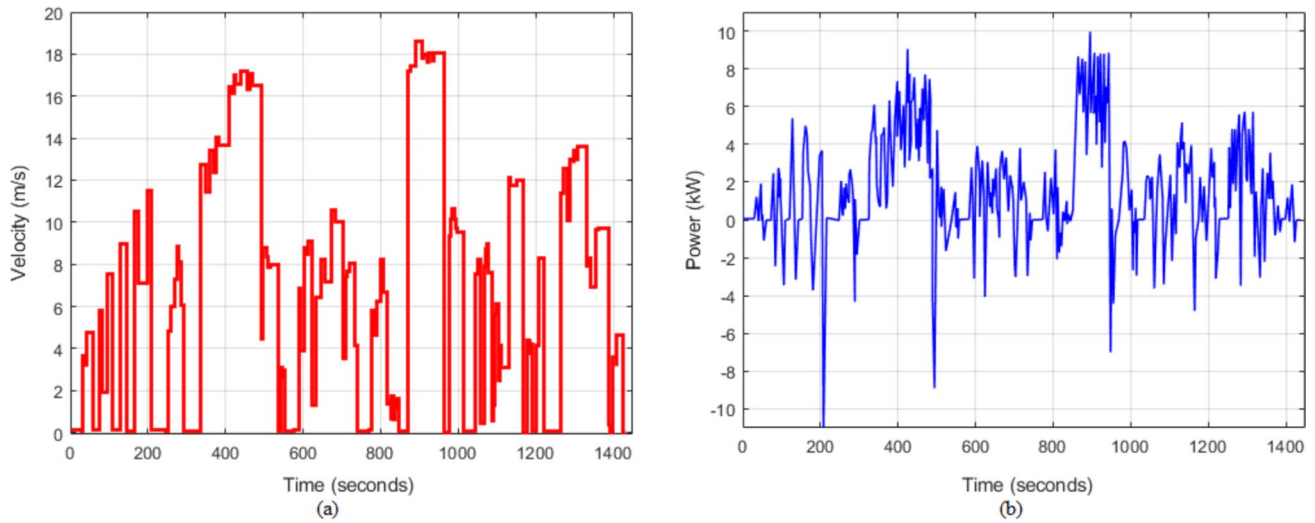

Fig. 11 Analyses of drive **a** velocity **b** demand power

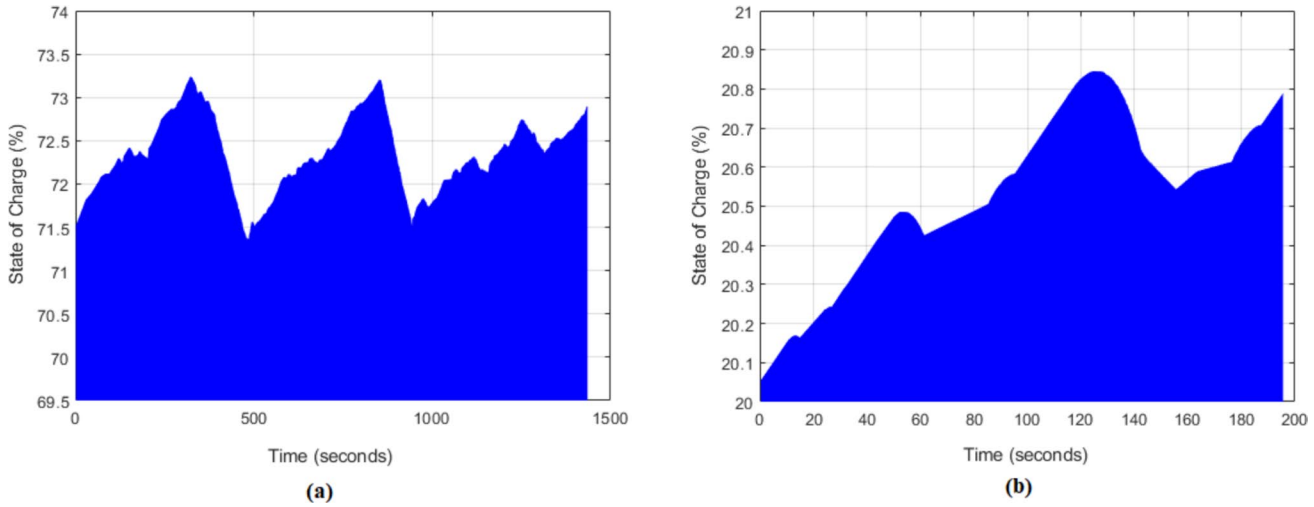

Fig. 12 Analyses of battery **a** SoC battery **b** SoC drive

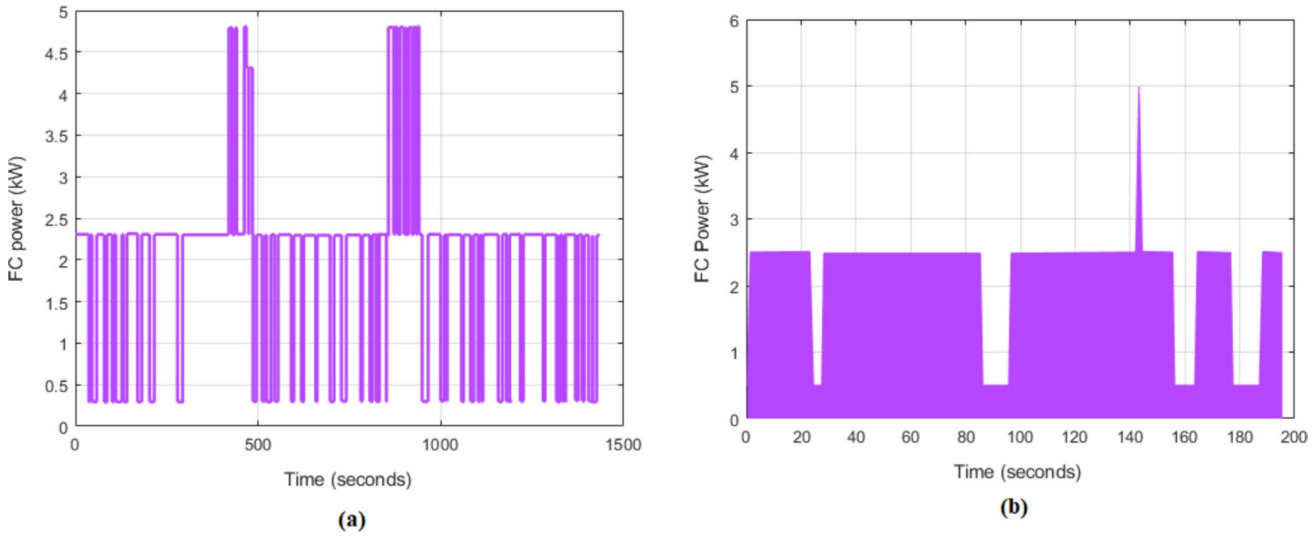

Fig. 13 Analyses of PEMFC system output power **a** PEMFC system **b** PEMFC drive system

helps keep the costs steady and avoids large fluctuations, which makes the system more reliable and cost-effective. Figure 16 presents a comparative analysis of optimization performance. In subplot 16(a), the effect of different population sizes (50, 100, 200, 300) on the loss convergence is depicted. It is observed that a population size of 50 leads to the fastest convergence with a significant drop in loss within the first 20 iterations, whereas larger populations such as 300 show slower but smoother convergence behavior. Subplot 16(b) depicts the effect of various learning rates (0.1, 0.01, and 0.001) on loss value reduction. A learning rate of 0.01 provides the most stable and fastest convergence to a lower loss, whereas higher and lower learning rates result in either overshooting or slower convergence. Subplot 16(c) compares the fitness convergence of the proposed method against existing algorithms such as SHO-CSGNN, PSO, SOA, and WHO. The proposed method demonstrates superior performance by achieving the lowest fitness value within fewer iterations, indicating its enhanced optimization capability and robustness.

This Table 2 compares the performance of the proposed EOO-SNN algorithm with several existing optimization algorithms: SHO-CSGNN, PSO, SOA, and WHO. The comparison is based on important performance indicators, including best fitness, mean fitness, and standard deviation. The proposed algorithm outperforms the others in terms of both fitness and computation time, with the best fitness score of 50 and no standard deviation, indicating consistent performance. In contrast, the existing methods show lower fitness values and some variability in their results.

Table 3 compares the sensitivity and performance of the proposed EOO-SNN algorithm with three existing

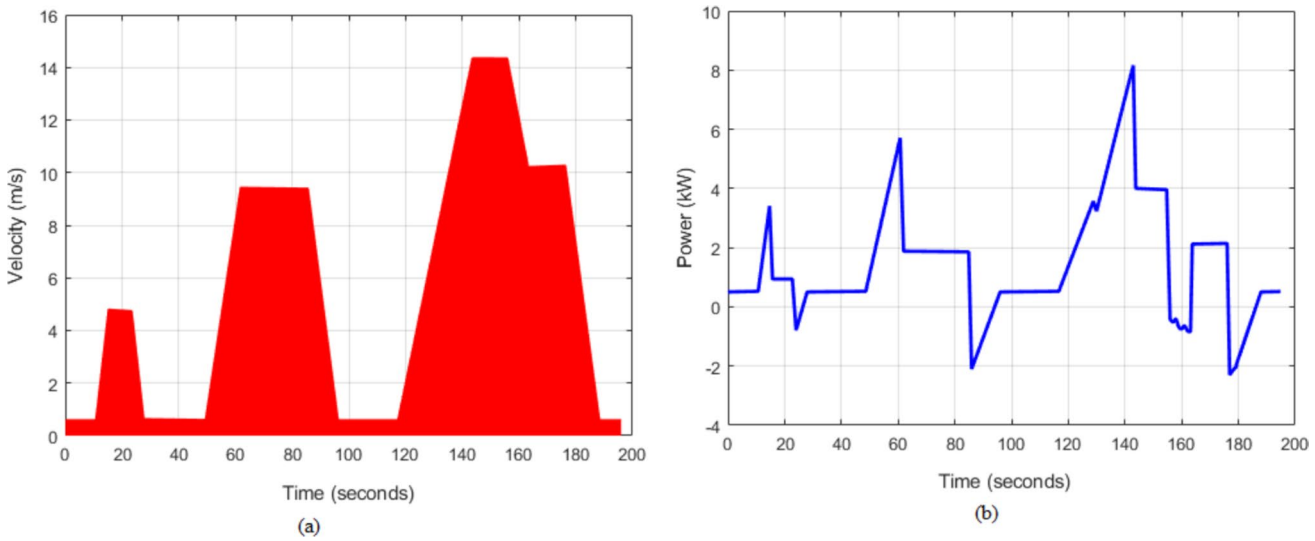

Fig. 14 Analyses of FC **a** drive velocity **b** demand power

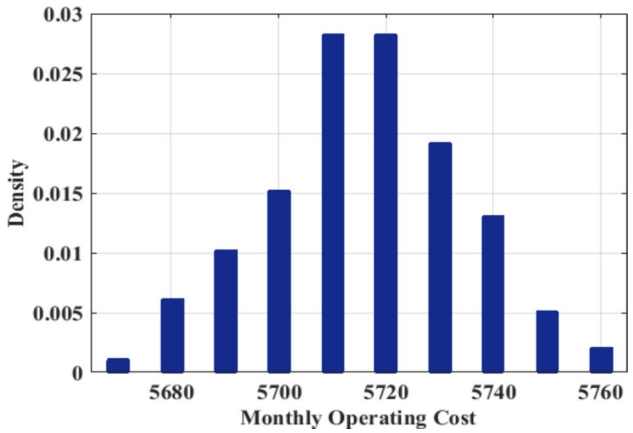

Fig. 15 Cost distribution under the proposed strategy

approaches (PSO, SOA and WHO). The metrics compared include charging station placement sensitivity, charging time sensitivity, charging efficiency under low demand, charging cost under high demand, and grid impact under high demand. The proposed EOO-SNN method shows the best performance across all metrics, particularly excelling in charging efficiency and grid impact reduction. It also has the lowest sensitivity values, indicating a more robust solution compared to existing techniques. Furthermore, the proposed approach has greater computational efficiency and requires the least amount of processing time.

Table 4 compares the proposed study with several existing optimization techniques for EV charging systems. The comparison includes efficiency, cost per kWh, fuel economy improvement, energy consumption, and environmental impact reduction. The proposed method achieves the highest efficiency (98.5%) and fuel economy improvement (12.50%), while maintaining the lowest cost per kWh (1.20). Additionally, it significantly reduces environmental impact by 35%. In comparison, existing techniques like Bi-directional LSTM and MADNN show lower performance in terms of both efficiency and environmental impact.

Table 5 compares the cost and efficiency of the proposed system with existing approaches. The proposed system has the lowest cost at $1.1 and the highest efficiency of 95%, making it the most cost-effective and efficient solution. In comparison, the PSO, SOA, and WHO systems have higher costs ($2.1, $3.1, and $4.1 respectively) and lower efficiencies, ranging from 85 to 92%. This highlights the proposed system's superior performance in both cost and efficiency.

5 Conclusion

This manuscript presents a novel Smart Charging for Fuel Cell Electric Vehicles (EVs) with Stochastic Network Planning using the Hybrid EOO-SNN approach. The main purpose of the proposed approach is to reduce charging costs, improve charging efficiency, and minimize the impact on the power grid. The method was excluded on the MATLAB platform and compared with existing strategies, demonstrating a significant improvement in efficiency, with the proposed system achieving a 45% efficiency increase, compared to 35% for PSO, 25% for SOA, and 15% for WHO. In terms of cost, the proposed strategy incurs a cost of $1.10/kWh, while PSO, SOA, and WHO cost $2.10, $3.10, and $4.10 per kWh, respectively. The system's overall cost is far cheaper than previous alternatives, making it a more cost-effective solution. Future research could focus on scaling the proposed optimization techniques to large-scale EV charging networks that account for varying geographical and socio-economic factors. Furthermore, integrating real-time

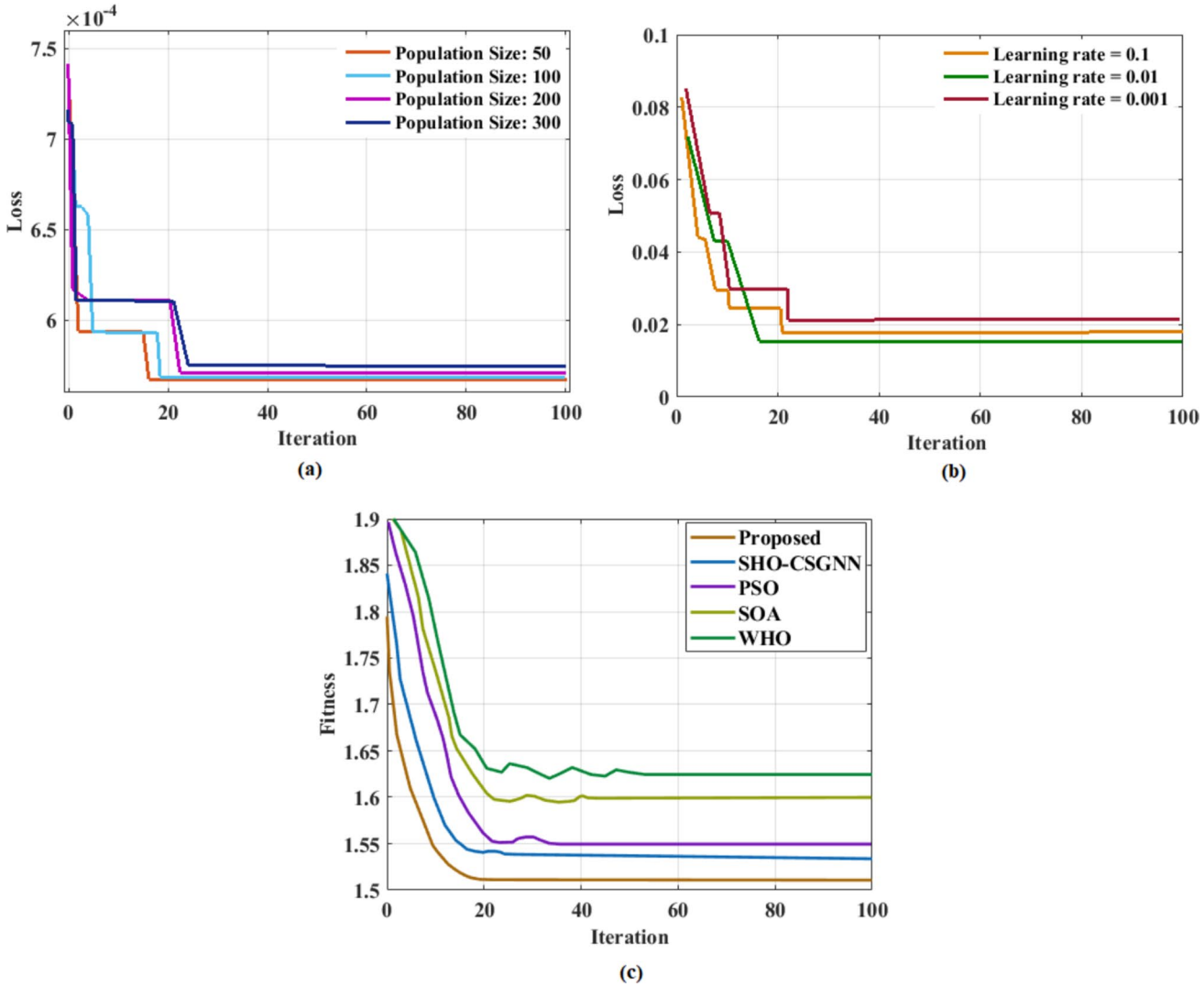

Fig. 16 Comparative analysis of optimization performance **a** population size **b** learning rate **c** convergence

Table 2 Performance comparison of different algorithms

Algorithm	Best fitness	Mean fitness	Std. Dev
Proposed (EOO-SNN)	50	50.000	0.000
SHO-CSGNN	48	48.167	0.211
PSO	46	46.833	0.547
SOA	44	44.750	0.683
WHO	45	45.667	0.471

data analytics and machine learning algorithms for adaptive energy management could optimize station utilization, reduce waiting times, and improve overall system performance. The exploration of evolving policy regulations, their impact on smart grid technologies, V2G interactions, and renewable energy integration will play an important part in ensuring the sustainability and resilience of EV charging infrastructure. Additionally, the development of hybrid

Table 3 Sensitivity and performance comparison of charging station placement and efficiency

Parameter	Proposed EOO-SNN	PSO	SOA	WHO
Charging station placement sensitivity (%)	± 5%	± 8%	± 6%	± 7%
Charging time sensitivity (%)	± 4%	± 7%	± 5%	± 6%
Charging efficiency under low demand (%)	90%	85%	88%	87%
Charging cost under high demand (%)	50%	55%	53%	56%
Grid impact under high demand (%)	25%	35%	30%	32%
Uncertainty sensitivity (%)	± 3%	± 8%	± 7%	± 10%
Computational efficiency (Time, sec)	45	60	70	65

Table 4 Comparative performance of proposed and existing EV charging optimization techniques

Technique and reference	Efficiency (%)	Cost ($/kWh)	Fuel economy improvement (%)	Energy consumption (kWh)	Environmental impact reduction (%)
Proposed study	98.5	1.20	12.50	350	35%
Bi-directional LSTM (B-LSTM) [17]	95.0	2.30	10.24	380	28%
Multi-agent deep neural network (MADNN) [18]	94.8	2.30	6.78	400	22%
Multi-objective robust optimization [19]	96.0	1.50	8.43	370	30%
Deep REINFORCE-based EMS for fuel cell HEVs [15]	97.0	1.75	7.68	365	32%
Stackelberg-based coordination for EV charging [21]	96.5	1.40	6.90	360	27%

Table 5 Cost and efficiency comparison of proposed and existing systems

System	Cost ($)	Efficiency (%)
Proposed system	1.1	95
PSO	2.1	92
SOA	3.1	89
WHO	4.1	85

optimization models that incorporate environmental, socio-economic, and technological factors could lead to more efficient and sustainable energy solutions in diverse settings.

Author contributions Dr. S. Dhas Bensam (Corresponding Author): Conceptualization, Methodology, Writing- Original draft preparation. Dr. K. S. Kavitha Kumari: Supervision Dr. Amarendra Alluri: Supervision Mr. P. Rajesh: Supervision.

Funding This study received no specific funds from public, commercial, or nonprofit funding agencies.

Data availability No datasets were generated or analysed during the current study.

Declarations

Competing interests The authors declare no competing interests.

Ethical approval consent to participate This article contains no research involving human subjects conducted by any of the writers.

References

1. Sabri, Y., & Hilmani, A. (2024). An IoT-Based 5G wireless sensor network employs a secure routing methodology leveraging DCNN processing. *Transactions on Emerging Telecommunications Technologies, 35*(12), Article e70025.
2. George, S. J., Ramaraju, S. K., Venkataraman, V., Kaliannan, T., Kumaravel, U., & Veerasundaram, M. (2022). Congestion management in deregulated power system by series facts device using heuristic optimization algorithms. *Journal of Intelligent & Fuzzy Systems, 42*(6), 6195–6208.
3. Wang, P., Wang, D., Zhu, C., Yang, Y., Abdullah, H. M., & Mohamed, M. A. (2020). Stochastic management of hybrid AC/DC microgrids considering electric vehicles charging demands. *Energy Reports, 6*, 1338–1352.
4. Muthamizh, S., Dheebanathan, A., Devanesan, S., & Vasugi, S. (2025). Improved photocatalytic and antibacterial properties by hydrothermally fabricate $CuWO_4$/PANI-Ppy nanocomposites. *Materials Science and Engineering: B*, *316*, 118141.
5. Xue, P., Xiang, Y., Gou, J., Xu, W., Sun, W., Jiang, Z., & Liu, J. (2021). Impact of large-scale mobile electric vehicle charging in smart grids: A reliability perspective. *Frontiers in Energy Research, 9*, 688034.
6. Sridharan, G., Babu, K. L., Ganapathy, D., Atchudan, R., Arya, S., & Sundramoorthy, A. K. (2023). Determination of nicotine in human saliva using electrochemical sensor modified with green synthesized silver nanoparticles using phyllanthus reticulatus fruit extract. *Crystals*, *13*(4), 589.
7. Xiang, Y., Wang, Y., Su, Y., Sun, W., Huang, Y., & Liu, J. (2020). Reliability correlated optimal planning of distribution network with distributed generation. *Electric Power Systems Research, 186*, Article 106391.
8. Xiang, Y., Meng, J., Huo, D., Xu, L., Mu, Y., Gu, C., & Teng, F. (2020). Reliability-oriented optimal planning of charging stations in electricity–transportation coupled networks. *IET Renewable Power Generation, 14*(18), 3690–3698.
9. Rahman, A. U., Ahmad, I., & Malik, A. S. (2020). Variable structure-based control of fuel cell-supercapacitor-battery based hybrid electric vehicle. *Journal of Energy Storage, 29*, Article 101365.
10. Yue, X., Ping, X., Yanliang, W., Lixiong, X., Wang, M., Miadreza, S. K., & Junyong, L. (2022). Robust expansion planning of electric vehicle charging system and distribution networks. *CSEE Journal of Power and Energy Systems, 10*(6), 2457–2469.
11. Merchant, A., Ganapathy, D. M., & Maiti, S. (2022). Effectiveness of local and topical anesthesia during gingival retraction: Anesthesia during cord packing. *Brazilian Dental Science*, *25*(1).
12. Borozan, S., Giannelos, S., & Strbac, G. (2022). Strategic network expansion planning with electric vehicle smart charging concepts as investment options. *Advances in Applied Energy, 5*, Article 100077.
13. Xia, F., Chen, H., Shahidehpour, M., Gan, W., Yan, M., & Chen, L. (2021). Distributed expansion planning of electric vehicle dynamic wireless charging system in coupled power-traffic networks. *IEEE Transactions on Smart Grid, 12*(4), 3326–3338.
14. Jian, P., Xiang, S., & Sabzalian, M. H. (2024). Planning of a charging station for electric and hydrogen vehicles under hydrogen storage and fuel cell systems using a novel stochastic p-robust optimization technique. *International Journal of Hydrogen Energy, 88*, 702–712.
15. Jouda, B., Al-Mahasneh, A. J., & Mallouh, M. A. (2024). Deep stochastic reinforcement learning-based energy management

strategy for fuel cell hybrid electric vehicles. *Energy Conversion and Management, 301*, Article 117973.
16. SivaramKrishnan, M., Kathirvel, N., Kumar, C., & Barua, S. (2024). Power management for fuel-cell electric vehicle using Hybrid SHO-CSGNN approach. *Energy Reports, 11*, 6069–6082.
17. Balakumar, P., Ramu, S. K., & Vinopraba, T. (2024). Optimizing electric vehicle charging in distribution networks: A dynamic pricing approach using internet of things and Bi-directional LSTM model. *Energy, 294*, Article 130815.
18. Aljafari, B., Jeyaraj, P. R., Kathiresan, A. C., & Thanikanti, S. B. (2023). Electric vehicle optimum charging-discharging scheduling with dynamic pricing employing multi agent deep neural network. *Computers and Electrical Engineering,105*, Article 108555.
19. Yao, Z., Wang, Z., & Ran, L. (2023). Smart charging and discharging of electric vehicles based on multi-objective robust optimization in smart cities. *Applied Energy, 343*, Article 121185.
20. Chatterjee, D., Biswas, P. K., Sain, C., Roy, A., Ahmad, F., & Rahul, J. (2024). Bi-LSTM predictive control-based efficient energy management system for a fuel cell hybrid electric vehicle. *Sustainable Energy, Grids and Networks, 38*, Article 101348.
21. Aljohani, T., Mohamed, M. A., & Mohammed, O. (2024). Tri-level hierarchical coordinated control of large-scale EVs charging based on multi-layer optimization framework. *Electric Power Systems Research, 226*, Article 109923.
22. Lan, T., Jermsittiparsert, K., Alrashood, T. S., Rezaei, M., Al-Ghussain, L., & Mohamed, A. M. (2021). An advanced machine learning based energy management of renewable microgrids considering hybrid electric vehicles' charging demand. *Energies, 14*(3), 569.
23. Khan, A. M., & Bagheri, M. (2024). Minimizing grid dependency and EV charging costs with PSO-based microgrid energy management. In *2024 IEEE East-West Design & Test Symposium (EWDTS)* (pp. 1–5). IEEE.
24. Lan, T., & Strunz, K. (2020). Modeling of multi-physics transients in PEM fuel cells using equivalent circuits for consistent representation of electric, pneumatic, and thermal quantities. *International Journal of Electrical Power & Energy Systems, 119*, Article 105803.
25. Sahin, H., & Esen, H. (2025). Performance and Energy Analysis of a Fuel Cell Electric Vehicle (November 2024). *IEEE Access*.
26. Radmanesh, H., & Gharibeh, H. F. (2024). Energy management of a fuel cell electric robot based on hydrogen value and battery overcharge control. *World Electric Vehicle Journal, 15*(8), 352.
27. Kirubadevi, S., Sathesh Kumar, T., S, S., & Venkata Krishna Reddy, C. (2024). Optimizing cost and emission reduction in photovoltaic–Battery-energy-storage-system-integrated electric vehicle charging stations: An efficient hybrid approach. *Energy Technology, 12*(7), 2301131.
28. Anastasiadis, A. G., Konstantinopoulos, S., Kondylis, G. P., & Vokas, G. A. (2017). Electric vehicle charging in stochastic smart microgrid operation with fuel cell and RES units. *International Journal of Hydrogen Energy, 42*(12), 8242–8254.
29. Salim, A., Jummar, W. K., Jasim, F. M., & Yousif, M. (2022). Eurasian oystercatcher optimiser: New meta-heuristic algorithm. *Journal of Intelligent Systems, 31*(1), 332–344.
30. Liu, C., Shen, W., Zhang, L., Du, Y., & Yuan, Z. (2021). Spike neural network learning algorithm based on an evolutionary membrane algorithm. *IEEE Access, 9*, 17071–17082.
31. Gharibeh, H. F., Yazdankhah, A. S., & Azizian, M. R. (2020). Energy management of fuel cell electric vehicles based on working condition identification of energy storage systems, vehicle driving performance, and dynamic power factor. *Journal of Energy Storage, 31*, Article 101760.

S. Dhas Bensam is currently working as an Assistant Professor in the department of Electrical and Electronics Engineering at V S B College of Engineering, Technical Campus, Coimbatore, Tamil Nadu, India. His research interests include Wind Energy, Special Electrical machines and in Optimization Techniques.

K. S. Kavitha Kumari is currently working as an Assistant Professor Grade -II, in the department of Electrical and Electronic Engineering, Aarupadai Veedu Institute of Technology, Vinayaka Mission's Research Foundation, Tamil Nadu, India. Her area of interest includes Smart grid, micro grid, Flexible AC Transmission systems and power system operation and control.

Amarendra Alluri He is currently working as Professor, Department of Electrical and Electronics Engineering, S R Gudlavalleru Engineering College, Andhra Pradesh. His research interests include Power System Security, Electric Vehicle, Cyber Security and Electromagnetic Propulsion.

P. Rajesh graduated from Anna University, India. He has more than 10 years of experience in research and development field. He has published more than 35 papers in international journals. His current research interests include artificial intelligence, power system, smart grid technologies and soft computing.